Dramatic Changes in the 3*s* Autoionization Process at the Beginning of the Ar I Sequence

P. van Kampen and G. O'Sullivan
Physics Department, University College Dublin, Belfield, Dublin 4, Ireland

V. K. Ivanov and A. N. Ipatov
St.-Petersburg State University, Polytekhnicheskaya 29, St.-Petersburg 195251, Russia

J. T. Costello and E. T. Kennedy
School of Physical Sciences, Dublin City University, Glasnevin, Dublin 9, Ireland
(Received 16 October 1996)

The $3s \rightarrow np$ resonances were observed to change dramatically in appearance with increasing ionization along the Ar I sequence, and within the $3s \rightarrow np$ channel of Ca^{2+}. By applying the Dyson equation method to positive ions for the first time, newly investigated double-electron processes were shown to play a crucial role in the interpretation of the resonance structure. The changes within the resonances result from their position relative to the Cooper minima in the 3*s* and 3*p* photoabsorption. [S0031-9007(97)02952-9]

PACS numbers: 32.80.Dz, 32.30.Jc

In recent years, photoionization of the outer *s*-subshell electrons in argon has attracted considerable interest [1–18], and a rather complete picture of 3*s* photoionization has been drawn from the $3s \rightarrow np$, $3s \rightarrow \varepsilon p$, and satellite spectra, both experimentally [2–8] and theoretically [9–18]. The cross sections of the individual processes are crucial since they depend strongly on electron correlation effects and therefore provide a sensitive test of modern theoretical and computational physics. Further valuable insight into these effects may be obtained by studying the evolution of inner shell excitation behavior along the isoelectronic sequence.

Very few data are available for the Ar-like ions K^+ and Ca^{2+} [19–23] because of the extreme difficulty of obtaining and maintaining a sufficient density of ions. Using a pioneering experimental technique of crossed ion and synchrotron radiation beams [24], Peart and Lyon measured the photoionization cross section of K^+ in the region of 3*s*-subshell excitations [21]. However, due to limited resolution, they were unable to discern profiles of any of the discrete structure observed, resulting in little insight into the detail of the photoionization process. In addition, possible weak structure at a photon energy of ~35.5 eV has been the subject of some controversy with conflicting views that it is either the $3s \rightarrow 4p$ resonance [22] or simply an experimental artifact [23].

This Letter reports the first high resolution inner shell photoabsorption spectra of K^+ and Ca^{2+} and shows that the behavior of the $3s \rightarrow np$ resonances differs radically from that in Ar. On moving from Ar to K^+, a striking *q*-reversal is observed for the $3s \rightarrow np$ transitions, while the resonances maintain a distinct windowlike appearance. In Ca^{2+} the main $3s \rightarrow 4p$ resonance almost disappears and the higher $3s \rightarrow np$ resonances have become almost symmetric absorption lines indicating a much weaker interaction with their associated εl continua.

From a theoretical viewpoint, a variety of calculations [7,14,15] have successfully reproduced the essential features of the Ar spectrum. In particular, the role of discrete double-electron excitations was explicitly stated in the work of Amusia and Kheifets [14]. However, we have found that their method is insufficient for an accurate description of the ionic spectra. Considerable extensions to this method are introduced in this Letter. The occurrence of *q*-reversals within a Rydberg series caused by interaction with a non-Rydberg level or an underlying "giant" or shape resonance has been discussed [25,26]. In the present case, we show that an additional mechanism for *q*-reversal can arise from the presence of Cooper minima [10] in the photoabsorption cross section.

Figure 1 shows the dramatic change in appearance of the $3s \rightarrow np$ resonances for Ar, K^+, and Ca^{2+}. The Ar spectrum was obtained by using a laser produced plasma of tungsten as a continuum source and argon gas as the absorber. The present results are in good agreement with those previously obtained in a synchrotron radiation experiment by Sorensen *et al.* [7]. The K^+ and Ca^{2+} spectra were produced using the dual laser plasma technique [27]. Briefly, a pair of plasmas, one of which forms the "sample" while the other constitutes the extreme ultraviolet (XUV) light source, are created by irradiating solid targets with high power focused laser pulses *in vacuo*. By a suitable choice of (i) sample target irradiance, (ii) time delay between the formation of the sample (jitter ± 2 ns) and backlighting plasmas, and (iii) path of the XUV beam through the sample plasma (spatial resolution ~200 μm), one can select the ion stage of interest to a high degree of purity. The spectral resolution is ~1500 at 60 eV rising to >2000 at 30 eV. Further details on the experiment are given in Ref. [28].

The K II spectrum was measured in the 33–48 eV region [Fig. 1(b)]. The spectrum shows no evidence

 0031-9007/97/78(16)/3082(4)$10.00

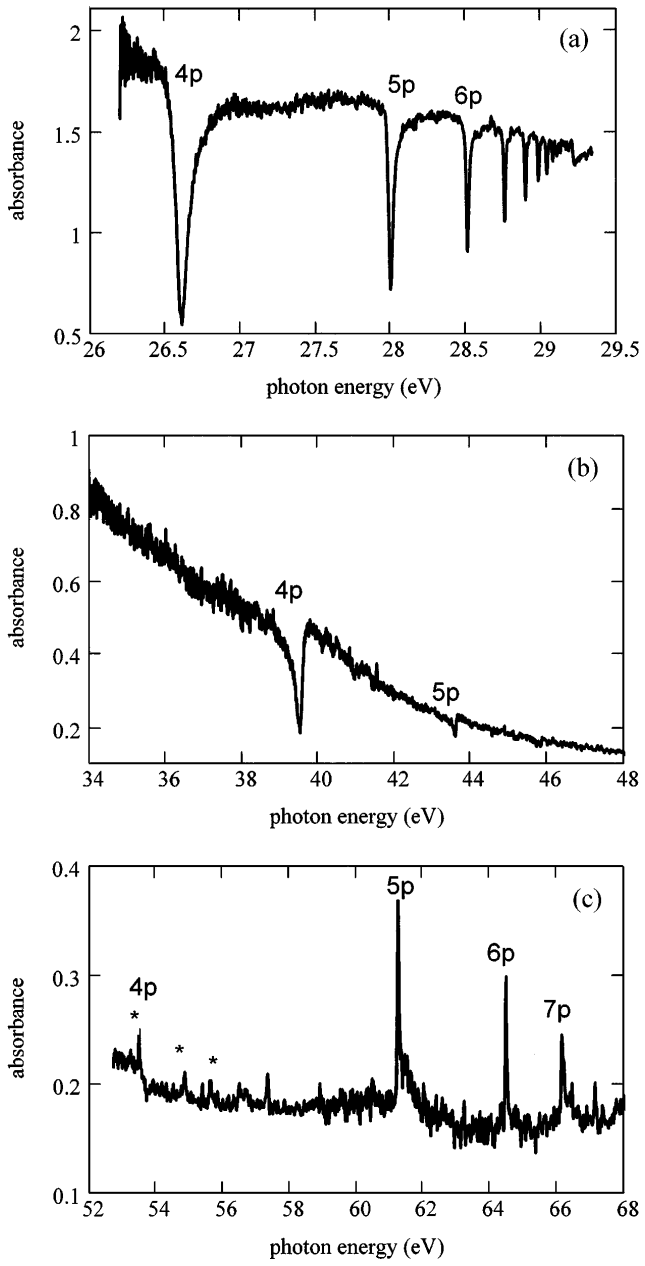

FIG. 1. The $3s \rightarrow np$ spectra of (a) Ar I, (b) K II, and (c) Ca III.

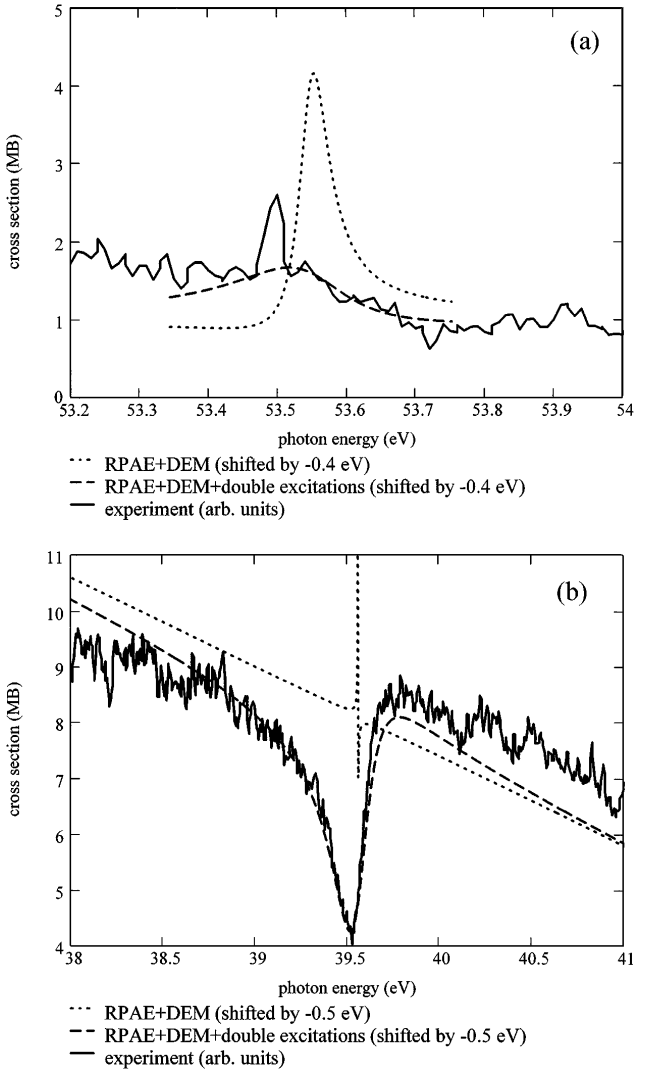

FIG. 2. Theoretical and experimental data for the $3s \rightarrow 4p$ transitions of (a) Ca III and (b) K II.

of the broad feature previously reported [21] in the 33–39 eV region, supporting the interpretation of Nasreen *et al.* [23] on this issue. All resonances observed are of the window type with the opposite sign of q in comparison with argon. A Fano profile was fitted to the $3s \rightarrow 4p$ resonance using the formula

$$\sigma = \sigma_0\left(1 - \rho^2 + \rho^2\frac{(q + \varepsilon)^2}{1 + \varepsilon^2}\right),$$

where $\varepsilon = (E - E_0)/\frac{1}{2}\Gamma$ (E is the photon energy, E_0 is the resonance energy, Γ is the resonance width) and the parameters ρ^2 and q describe the shape of the resonance. The $3p$ continuum was assumed to decrease linearly with photon energy in the region around the resonance [cf. Fig. 1(b)]. We obtain fitted Fano parameters $q = 0.4 \pm 0.1$, $E_0 = 39.56 \pm 0.05$ eV, and $\Gamma = 0.19(+0.02/-0.08)$ eV.

In the spectrum of Ca III [Fig. 1(c)], the $3s \rightarrow 4p$ resonance is obviously very different from the $3s \rightarrow np$ resonances. It is very wide and diffuse [see Fig. 2(a)] and has a q value of about -1, while the other resonances are narrow absorption-type features with high q. Energy levels and quantum defects are listed in Table I. The ratio of the intensities of the weak features [marked $*$ in Fig. 1(c)] to the $3s \rightarrow 5p/6p$ resonances vary with laser power density, indicating clearly that these originate from a different charge state.

The measured energies differ by up to 0.2 eV from those already reported in the literature [19,20]; cf. Table I. Corroboration of our assignments comes from isoelectronic comparison and Rydberg series expansion. The series limit, $I_{3s} = I_{3p} + E(3s\,3p^6)$, is 47.82 eV for the K II series, and 69.81 eV for Ca III [29].

TABLE I. Experimental and calculated energy levels (in eV) and quantum defects of the $3s \rightarrow np$ transitions in K II and Ca III. E^{R} = RPAE energy, E^{RD} = RPAE + DEM.

Ion	n	E_{exp}	E_{lit}	E^{R}	E^{RD}	δ
K II	4	39.56 ± 0.05	39.64 [20]	45.39	39.94	1.44
	5	43.61 ± 0.03	...	49.29	44.09	1.41
Ca III	4	53.63 ± 0.10	53.447 [19]	59.77	54.06	1.26
	5	61.27 ± 0.05	61.104 [19]	67.16	61.85	1.21
	6	64.50 ± 0.05	...	70.33	65.02	1.20
	7	66.18 ± 0.05	...	71.99	66.68	1.20
	8	67.16 ± 0.05	...	72.97	67.66	1.21

Calculations of the autoionizing structure in the $3p$ photoabsorption spectra of K^+ and Ca^{2+} associated with $3s \rightarrow np$ excitations have been performed using *ab initio* methods based on many-body theory. Starting from the Hartree-Fock (HF) approximation, many-electron correlations were taken into account using the following approaches: the random phase approximation with exchange (RPAE) for calculation of phototransition amplitudes [30], the Dyson equation method (DEM) for energy shifts (the self-energy part) and corrections to wave functions of ground and discrete excited states [31,32], and many-body perturbation theory for corrections to the photoamplitudes due to double-electron processes.

The calculations indicate that the changes in profile are a direct result of a change in the positions of the 3*s* and 3*p* Cooper minima (CM). In Ar, all 3*s* resonances lie below both CM. In K^+, the 3*s* CM lies in the discrete spectrum but the 3*p* CM lies above all 3*s* resonances; this explains the consistent q parameters and the extreme weakness of the $3s \rightarrow np$ transitions. In Ca^{2+}, the 3*s* CM has moved below the discrete resonances while the 3*p* CM lies just after the 4*p* resonance, causing a change in the imaginary part of the $3s \rightarrow 4p$ amplitude and hence in q. Calculations for Sc^{3+} indicate that the 3*s* spectrum lies above both CM.

The results of the calculations within the different approximations, presented in Table II, are therefore very sensitive to the energy positions of the discrete excitations relative to the CM in the $3s \rightarrow \varepsilon p$ partial cross section, leading to incorrect values for the Fano profile parameters within conventional RPAE; see Table II. Taking into account double-electron excitations shifts the position of the CM relative to the $3s \rightarrow np$ excitations, and also affects the resonance widths significantly.

To improve the transition energies and discrete state wave functions we have used DEM [32], where the wave function ψ_{nl} describing a bound electron with energy E_{nl} satisfies the following integral equation:

$$\hat{H}^{(0)}\psi_{nl}(\vec{r}) + \int \Sigma_{E_{nl}}(\vec{r},\vec{r}\,')\psi_{nl}(\vec{r}\,')\,d\vec{r}\,' = E_{nl}\psi_{nl}(\vec{r})\,. \tag{1}$$

Here $\hat{H}^{(0)}$ is the static HF Hamiltonian of the ion and $\Sigma_E(\vec{r},\vec{r}\,')$ is the self-energy part of the single-electron Green function, which plays the role of an energy-dependent nonlocal potential. The latter was calculated in the second order of perturbation theory, as in Refs. [30–32], for ground state 3*s* and 3*p* electrons with transferred momentum $\Delta l = 0, 1, 2, 3$; the largest contributions come from terms with $\Delta l = 0, 1$. Equation (1) includes the dynamical polarization interaction between the electron under consideration and the other electrons in the ion.

By solving Eq. (1) with the calculated self-energy part we have obtained new energies and wave functions for the 3*s* and 3*p* electrons, which have been used within RPAE to take into account the interchannel and polarization interaction simultaneously. The calculated energies are presented in Table I. Thus, within RPAE + DEM, the 3*s*-electron energy shift in Ca^{2+} is equal to 5.3 eV, the oscillator strength $f = 0.0058$, $q \approx 4.9$, and width $\Gamma \approx 0.051$ eV (see Table II). The remaining $3s \rightarrow np$ resonances of the series are obtained with the sign of the q-parameter reversed. Although the calculated energies for the $3s \rightarrow np$ transitions agree quite well with experiment (applying an energy shift of about 0.5 eV), the shape of the $3s \rightarrow 4p$ resonance is not reproduced within RPAE + DEM.

This disagreement is associated with double-electron excitations, transitions to which are predicted to have large oscillator strengths and to lie very close to the $3s \rightarrow np$ excitations. The present calculations are performed in

TABLE II. Parameters for the $3s \rightarrow np$ transitions in K^+ and Ca^{2+}.

Transition	RPAE		RPAE + DEM			Double-electron + RPAE + DEM				Experiment	
	q	Γ (eV)	q	Γ (eV)	ρ^2	q	f	Γ (eV)	ρ^2	q	γ (eV)
						K II					
$3s \rightarrow 4p$	−2.2	0.0014	−49	.000 05	0.066	0.37	0.034	0.23	0.472	0.4 ± 0.1	0.19 + 0.02/ − 0.08
$3s \rightarrow 5p$	4.1	0.003	−1.0	0.003	0.256	0.53	0.024	0.056	0.358	0.5 ± 0.2	0.05 ± 0.03
						Ca III					
$3s \rightarrow 4p$	54	0.035	4.9	0.052	0.127	−3.2	0.0042	0.20	0.065	−1	0.3 ± 0.1
$3s \rightarrow 5p$	−9.1	0.021	−12	0.029	0.073	7.6	0.0060	0.033	0.165		0.06 ± 0.03
$3s \rightarrow 6p$	−7.1	0.012	−7.5	0.016	0.183	7.2	0.0040	0.012	0.302		0.05 ± 0.03
$3s \rightarrow 7p$	−6.5	0.0070	−6.6	0.0094	0.232	7.6	0.0026	0.006	0.345		0.04 ± 0.03

the lowest order of perturbation theory with the same set of corrected energies and wave functions as before. The main contribution from double-electron processes describing the amplitudes of the $3s \rightarrow np$ resonance transitions comes from the following diagrams.

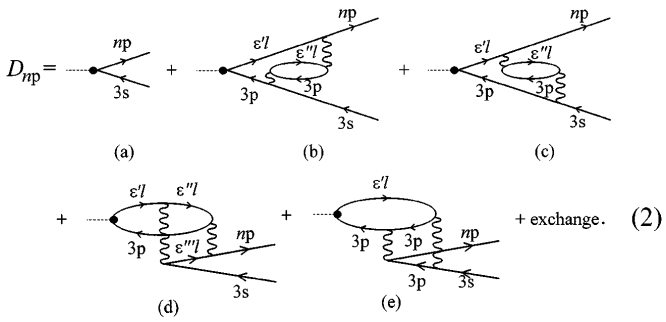

(2)

The lines marked with an arrow to the left (right) correspond to the electron wave functions of the ground (excited) states, while the dashed lines indicate the incoming photon and wavy lines denote the Coulomb interaction. In the above diagrams, all RPAE and exchange interactions are included in the dots at the vertices and all wavy lines, respectively. The calculations of these amplitudes have been performed with complete summation and integration over the discrete and continuum spectra. As in Ar [14], the main contribution to the amplitudes comes from the double-electron discrete excitations (2c) and (2e). However, the εd and εs continua also make significant contributions in all diagrams (2b)–(2e) and cannot be neglected in the calculations.

From Table II and Fig. 2(a) one can see that the double-electron correlations dramatically affect the Fano parameters of all resonances. In particular, the width of the Ca^{2+} $3s \rightarrow 4p$ resonance increases by a factor of 4 and the q-parameter changes sign. Because of this effect, and the relatively small value of the ρ^2 parameter, the $3s \rightarrow 4p$ transition appears as a very smooth structure in the $3p$ photoabsorption continuum. The remaining $3s \rightarrow np$ transitions are also sensitive to double-electron excitations which here change the sign of q. However, they appear to retain the same character with relatively small widths.

Inclusion of double-electron correlations also allows us to describe the window-type $3s \rightarrow np$ resonances in the K^+ photoabsorption spectrum. Thus, instead of a sharp and narrow $3s \rightarrow 4p$ resonance with large q-parameter ($\Gamma = 0.5$ meV, $q = -49$) within RPAE, we obtain a window-type profile with $q = 0.37$ and $\Gamma = 0.23$ eV [see Fig. 2(b)]. The newly calculated Fano parameters are in excellent agreement with the experimental values; see Table II and Fig. 2(b).

In conclusion, the $3s \rightarrow np$ resonance structure is observed to change dramatically in appearance both with increasing ionization along the argonlike sequence and within the $3s \rightarrow np$ channel of Ca^{2+}, and newly investigated double-electron processes have been shown to play a crucial role in the interpretation of the observed structure.

This work was supported by the Irish Science and Technology Agency, FORBAIRT, under Grants No. SC/95/403 and No. SC/95/483 and the European Union under Contract No. CHRX-CT93-0361. V. K. I. and A. N. I. are thankful to J. B. West for useful discussions, to University College Dublin, the Royal Society, and the Russian Fund of Fundamental Investigation (Grant No. 95-02-05562-a) for the support of the present work.

[1] V. Schmidt, Rep. Prog. Phys. **55**, 1483 (1992).
[2] R. P. Madden and K. Codling, Phys. Rev. Lett. **10**, 516 (1963).
[3] R. P. Madden, D. L. Ederer, and K. Codling, Phys. Rev. **177**, 136 (1969).
[4] J. A. R. Samson and J. L. Gardner, Phys. Rev. Lett. **33**, 671 (1974).
[5] K.-H. Schartner *et al.*, Phys. Rev. Lett. **61**, 2744 (1988).
[6] M. A. Baig and M. Ohno, Z. Phys. D **3**, 369 (1986).
[7] S. L. Sorensen *et al.*, Phys. Rev. A **50**, 1218 (1994).
[8] A. A. Wills *et al.*, J. Phys. B **22**, 3217 (1989).
[9] U. Fano, Phys. Rev. **124**, 1866 (1961).
[10] J. W. Cooper, Phys. Rev. **128**, 681 (1962).
[11] U. Fano and J. W. Cooper, Phys. Rev. **137**, A1364 (1965).
[12] M. Ya. Amusia *et al.*, Phys. Lett. **40A**, 361 (1972); J. Exp. Theor. Phys. **66**, 1537 (1974).
[13] P. G. Burke and K. J. Taylor, J. Phys. **8**, 2620 (1975).
[14] M. Ya. Amusia and A. S. Kheifets, Phys. Lett. **82A**, 407 (1981).
[15] V. V. Balashov *et al.*, Opt. Spectrosc. **49**, 577 (1980).
[16] A. Hibbert and J. E. Hansen, J. Phys. B **20**, L245 (1987).
[17] V. L. Sukhorukov *et al.*, Phys. Lett. A **169**, 445 (1992).
[18] W. Wijesundera and H. P. Kelly, Phys. Rev. A **39**, 634 (1989).
[19] S. O. Kastner *et al.*, Phys. Rev. A **16**, 577 (1977).
[20] H. Aizawa *et al.*, J. Phys. B **18**, 189 (1985).
[21] B. Peart and I. C. Lyon, J. Phys. B **20**, L673 (1987).
[22] R. D. Cowan and M. Wilson, J. Phys. B **21**, L201 (1988).
[23] G. Nasreen, P. C. Deshmukh, and S. T. Manson, J. Phys. B **21**, L281 (1988).
[24] I. C. Lyon *et al.*, J. Phys. B **19**, 4137 (1986).
[25] J. P. Connerade and A. M. Lane, J. Phys. B **20**, 1757 (1987).
[26] J. P. Connerade, A. M. Lane, and M. A. Baig, J. Phys. B **18**, 3507 (1985).
[27] J. T. Costello *et al.*, Phys. Scr. **T34**, 77 (1991).
[28] E. T. Kennedy *et al.*, Opt. Eng. **33**, 3984 (1994).
[29] J. Sugar and C. Corliss, J. Phys. Chem. Ref. Data **14**, Suppl. 2 (1985).
[30] M. Ya. Amusia, *Atomic Photoeffect* (Plenum Press, New York, 1990).
[31] L. V. Chernysheva *et al.*, J. Phys. B **21**, L419 (1988).
[32] P. Dunne, G. O'Sullivan, and V. K. Ivanov, Phys. Rev. A **48**, 4358 (1993).